

Intermediate water circulation drives distribution of Pliocene Oxygen Minimum Zones

Received: 5 May 2022

Accepted: 17 November 2022

Published online: 04 January 2023

 Check for updatesCatherine V. Davis ¹✉, Elizabeth C. Sibert ^{2,3}, Peter H. Jacobs ^{4,7},
Natalie Burls ⁵ & Pincelli M. Hull ^{2,3,6}

Oxygen minimum zones (OMZs) play a critical role in global biogeochemical cycling and act as barriers to dispersal for marine organisms. OMZs are currently expanding and intensifying with climate change, however past distributions of OMZs are relatively unknown. Here we present evidence for widespread pelagic OMZs during the Pliocene (5.3–2.6 Ma), the most recent epoch with atmospheric CO₂ analogous to modern (~400–450 ppm). The global distribution of OMZ-affiliated planktic foraminifer, *Globorotaloides hexagonus*, and Earth System and Species Distribution Models show that the Indian Ocean, Eastern Equatorial Pacific, eastern South Pacific, and eastern North Atlantic all supported OMZs in the Pliocene, as today. By contrast, low-oxygen waters were reduced in the North Pacific and expanded in the North Atlantic in the Pliocene. This spatially explicit perspective reveals that a warmer world can support both regionally expanded and contracted OMZs, with intermediate water circulation as a key driver.

The presence and distribution of low-oxygen water masses are of global importance to biogeochemical and nutrient cycling and may present a barrier for many marine organisms^{1–7}. A link between anthropogenic climate change and marine deoxygenation has become clear over the past decades, with growing evidence for an expansion of oxygen minimum zones (OMZs) and coastal hypoxia^{4,6,8–11}. Oxygen minimum zones can be broadly defined as open ocean, mid-waters with oxygen content markedly lower than the surface, usually reaching greatest intensity between 200 and 1000 m depth. Quantitative definitions vary widely between publications. As most paleo-oxygen proxies are not quantitative we converge upon a qualitative definition of an OMZ as a region of subsurface dissolved oxygen levels low enough to effect biological or chemical gradients. Although the extent and intensity of OMZs fluctuate on decadal to millennial time scales^{12–16}, the future distribution of marine oxygenation in a warmer climate remains unclear. This is because long-term, secular changes in

the distribution of OMZs depend on the complex interplay of multiple factors that include global and local shifts in intermediate water circulation, stratification, export productivity and remineralization, and ocean temperatures, the balance among which is not well understood.

In such complex systems, combining modeling and data-driven approaches offers a powerful tactic for disentangling the relative importance and interactions of potential drivers under different boundary conditions. For instance, modern OMZs are frequently associated with regions where surface productivity is high and ventilation of intermediate source waters is low, typified by Eastern Boundary Upwelling Systems (EBUSs)¹⁷ (Fig. 1). However, the degree to which OMZs have been retained in, or confined to, these types of environments under conditions of both variable productivity and ventilation has not been widely explored. Here we investigate OMZs during the Pliocene Epoch (5.3–2.6 million years ago; Ma). The mid-Piacenzian, also known as the mid-Pliocene Warm Period (~3 Ma), has

¹Department of Marine, Earth, and Atmospheric Sciences, North Carolina State University, Raleigh, NC, USA. ²Department of Earth and Planetary Sciences, Yale University, New Haven, CT, USA. ³Yale Institute for Biospheric Studies, Yale University, New Haven, CT, USA. ⁴Department of Environmental Science and Policy, George Mason University, Fairfax, VA, USA. ⁵Department of Atmospheric, Ocean & Earth Sciences, George Mason University, Fairfax, VA, USA. ⁶Yale Peabody Museum of Natural History, Yale University, New Haven, CT, USA. ⁷Present address: Earth Science Division, NASA Goddard Space Flight Center, Greenbelt, MD, USA. ✉e-mail: catherinedavis@ncsu.edu

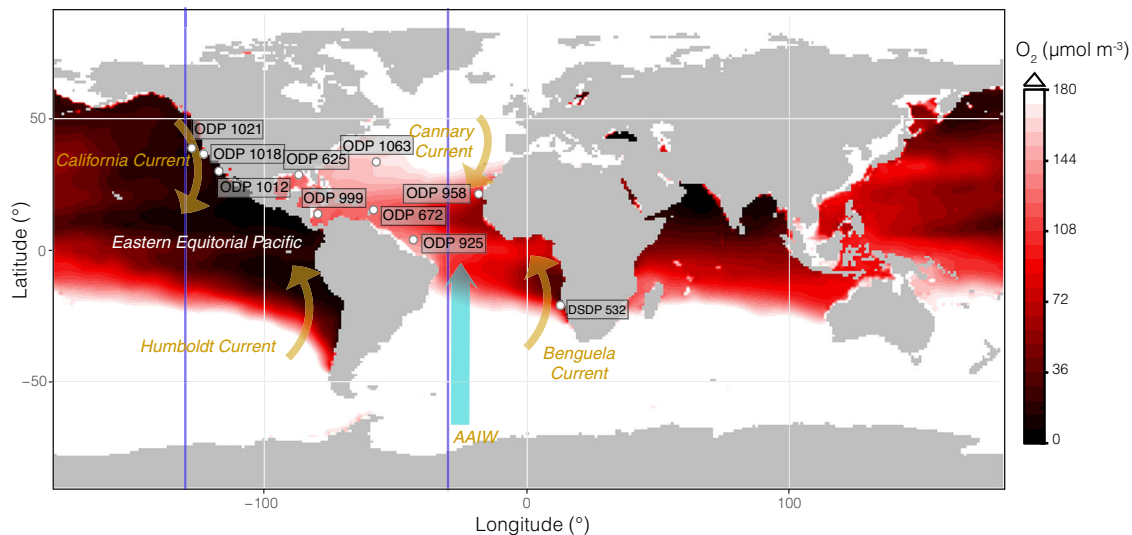


Fig. 1 | Distribution of low-oxygen mid-waters in the modern ocean. Minimum O_2 within the upper 1000 m from WOA18 data (1955–2010)⁹⁰ is shown with lower O_2 concentrations in darker red. Regions where oxygen concentrations do not fall below $172 \mu\text{mol m}^{-3}$ are white. Dark blue lines show the location of sections

expanded in Fig. 5. Key surface currents are shown in orange and Antarctic Intermediate Water (AAIW) in light blue. All core sites discussed in the text are shown as white points. A Pliocene comparison is available as Supplementary Fig. 7.

received particular interest as the most recent period during which atmospheric CO_2 was comparable to present ($\sim 400\text{--}450 \text{ ppm}^{18\text{--}20}$), with global mean temperatures $\sim 2\text{--}3^\circ\text{C}$ warmer than the 21st century^{21–23}. As a result, the Pliocene has been the focus of multiple generations of the Pliocene Research, Interpretation and Synoptic Mapping (PRISM) project and several major data-model studies comparing PRISM reconstructions to Pliocene climate model simulations like the Pliocene Model Intercomparison Project (PlioMIP)^{23,24}.

Despite the similarities in pCO_2 and continental configurations between the mid-Piacenzian and modern, there were several key differences in Pliocene oceans that have the potential to impact the extent, intensity, and distribution of OMZs. This includes the presence of distinct ocean circulation patterns, such as a Pacific Meridional Overturning Circulation (PMOC), which has no modern analogue^{25,26} but could affect the distribution and age of intermediate water masses. Some models of Pliocene-like climate suggest globally reduced upwelling-conductive winds due to reduced meridional temperature gradients^{27,28}. This could act to reduce nutrient input and export productivity and decrease the strength and extent of OMZs especially in EBUSs. Empirical evidence for this last scenario is mixed, with nitrogen isotopes indicating a reduction in productivity in both the Benguela^{29,30} and California Current systems³¹, but with increased calcium carbonate mass accumulation rates also observed in the California Current³². Meanwhile, warmer surface and intermediate waters in the Pliocene would have decreased oxygen solubility, potentially countering the effect of reduced upwelling and promoting expanded OMZs. In addition, while paleogeography by the end of the Piacenzian closely resembled today's continental configuration, the influence of the closure of the Central American Seaway during the Pliocene on North Atlantic circulation is poorly constrained³³.

To date, both data and model-based reconstructions of OMZ distributions in the fossil record have been limited due to a paucity of relevant model outputs and empirical constraints. On the modeling side, the inclusion of biological processes within paleoclimate simulations using full-complexity general circulation models is in its infancy. On the data side, there is a dearth of OMZ proxies for water column oxygenation, with most proxies restricted to benthic environments. As a result, past studies have frequently been limited to time periods and locations where the OMZ intersects the seafloor or pelagic anoxia (no oxygen) is extreme enough for indicators of euxinic (anoxic

and sulfidic) conditions to be deposited in marine sediments. Some examples of proxy-based OMZ reconstructions include deglacial expansion along continental margins¹⁵ and references therein) and the identification of water column euxinia during the Mesozoic Oceanic Anoxic Events^{34–36}. However, because OMZs are mid-water phenomena, they are primarily pelagic, rendering them frequently invisible to benthic proxies. Moreover, most modern OMZ waters are not truly anoxic (Fig. 1), much less euxinic. While there are a few additional proxies for pelagic OMZs, such as nitrogen isotopes and organic carbon accumulation, they are responsive to a suite of factors, such as nutrient utilization and preservation frequently making it difficult to tease apart the influence of the various drivers without additional context.

Here we present the distribution of *Globorotaloides hexagonus*, a deep-dwelling, OMZ-associated planktic foraminifera³⁷, as a proxy for pelagic OMZs. *Globorotaloides hexagonus* has been found at a range of depths ($\sim 50\text{--}1000 \text{ m}$) and productivity regimes and is consistently associated with sub-thermocline low-oxygen waters (Fig. 2a)^{37–40}. By leveraging extensive databases of the distribution of planktic foraminifera in modern and mid-Pliocene oceans^{41–43}, Species Distribution Models (SDM), and a biogeochemically enabled global climate simulation resembling Pliocene conditions^{25,44,45}, we provide both data-based and model-based constraints on pelagic OMZs in the Pliocene and investigate the dominant drivers of changed OMZ distributions.

Results & discussion

Ecological modelling and proxy interpretations of *G. hexagonus*

Ecological modeling of *G. hexagonus* in the modern ocean supports an association with dissolved oxygen levels at sub-thermocline depths, with results presented here for $400\text{--}800 \text{ m}$ integrated depth (Fig. 3). Species Distribution Models performed best when using multiple correlated variables (O_2 , temperature, salinity, and macronutrients SiO_3 , PO_4 , and NO_3). Dissolved oxygen consistently ranked among the most important of these variables, and temperature and salinity among the least important for predicting habitat. After oxygen, silica was the next most important variables at depth followed by phosphate, but both were far less important for models calibrated using surface (0 m) parameters. This effectively demonstrates an affinity of *G. hexagonus* for low oxygen mid-waters, decoupled from surface productivity. We note that the term 'mid-water' is used here to

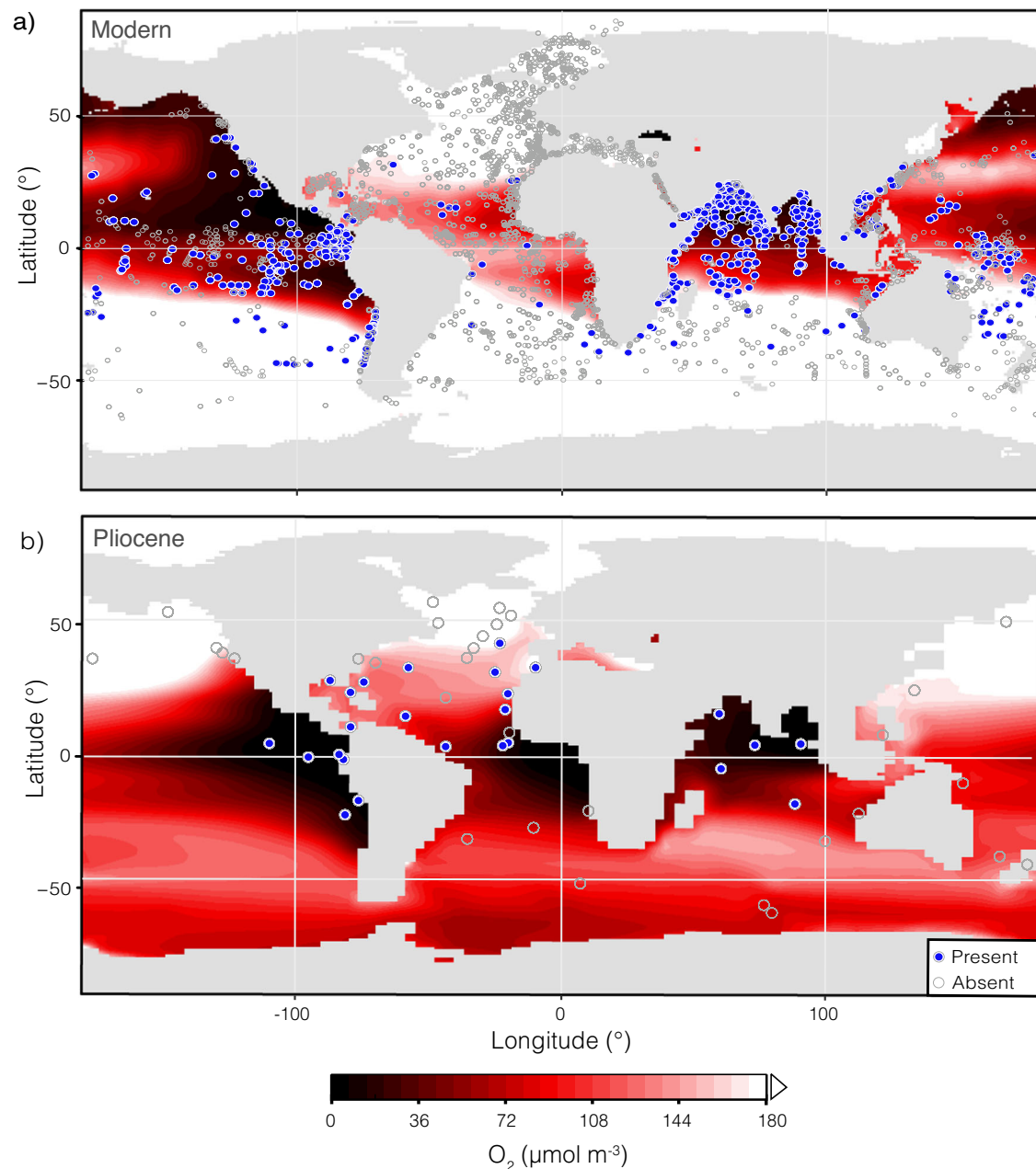


Fig. 2 | Distribution of low-oxygen affiliated planktic foraminifer *G. hexagonus* and oxygen at -600 m in the modern and Pliocene oceans. Oxygen concentrations at -600 m depth **a)** aggregated from WOA18 data (1955-2010)⁹⁰, and **b)** from the Pliocene-like CEM simulation. Sites where *G. hexagonus* was found to be

present are shown with blue fill; sites where *G. hexagonus* was absent are open gray points^{37-40,82-87}. Lower O_2 concentrations are shown in darker red and oxygenation above $172 \mu\text{mol m}^{-3}$ is white.

describe depths from the thermocline to -1000 m as distinct from 'intermediate water'. While the later frequently references specific water masses (e.g., 'Antarctic Intermediate Water'), both *G. hexagonus* and OMZs may occupy depth ranges not limited to named intermediate water masses.

Species Distribution Models driven by observed ocean conditions confirm the strong relationship between the presence of *G. hexagonus* and low oxygen mid-waters, demonstrating high AUC (0.87; true positive rate versus false positive rate) and percentage correct (84%) prediction scores. Models using dissolved oxygen alone avoid potential overfitting and performed well even compared to those fit with all environmental covariates (Supplementary Table 1). Whether a specific oxygen threshold within the OMZ is required to maintain a population of *G. hexagonus* is currently unresolved. The only published work

comparing water-column oxygenation with the depth distribution and abundance of *G. hexagonus* found the species to be most abundant in waters with oxygen below 0.14 ml L^{-1} ($-9 \mu\text{mol m}^{-3}$) in the Eastern Tropical North Pacific, but individuals were found at low densities throughout and just above the oxycline³⁷. This may be taken as a guide to the species' oxygen range, but whether the same oxygen levels predict population abundance and depth distributions globally will require additional sampling.

The preferred oxygen-only SDM indicates almost no viable habitat for *G. hexagonus* in the modern Atlantic Ocean, in line with sparse reported (and disputed), occurrences in the basin (Figs. 2a and 3a) and suggests that the species may be present only as small, restricted populations in the Atlantic. The SDM does predict suitable habitat for *G. hexagonus* in the subpolar North Pacific (Fig. 3a),

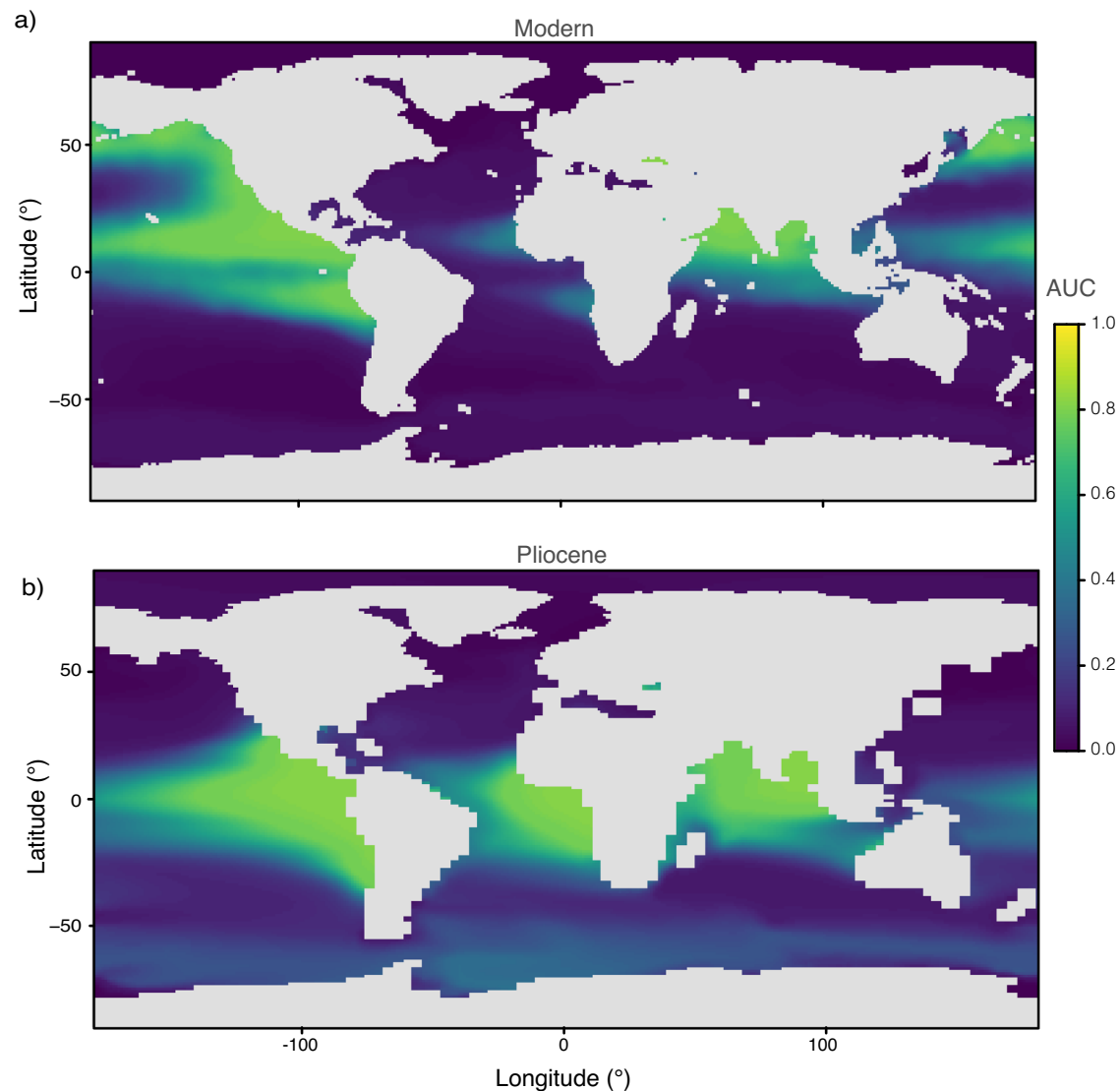


Fig. 3 | Oxygen-based SDMs showing suitable habitat for *G. hexagonus* in the modern and Pliocene Ocean. Habitat is predicted from **a)** WOA18 oxygen data (1955–2010)⁹⁰ integrated between 400 and 800 m, and **b)** oxygen outputs

integrated between 400 and 800 m in the Pliocene-like climate simulation. AUC (true positive rate versus false positive rate) ranges between 0 and 1, with 1 indicating perfect prediction by the model.

where it has not been observed in modern samples. It is possible that *G. hexagonus* may be present in this environment but not yet identified, though we think it more likely that their habitat is geographically limited to tropical to transitional zones. Geographic range limits are common for planktic foraminifera, with few truly cosmopolitan species⁴⁶, and our SDM model only accounted for observations (and not absences) given the low detection probability of rare species (e.g., Fig. 2a). Thus, the range of *G. hexagonus* may be bounded by additional geographic or hydrologic constraints, which are not resolved given the modeling approach used. A greater understanding of the ecology and biogeographic limitations of *G. hexagonus* along with alternate modeling approaches will serve to improve future proxy interpretations.

A proxy is definitionally an indirect measure, and paleoceanographic studies are at their strongest when proxy limitations are accounted for and multiproxy or combined proxy-model approaches with different underlying biases and limitations are used. Here we discuss the peculiarities and limitations of the use of *G. hexagonus* as OMZ proxy in terms of “false positives” and “false negatives” given our use of a binary presence/absence metric. For *G. hexagonus*, a false positive can occur through misidentification, lateral transport, or

incongruity in timescales of oxygen measurements and species occurrence data (Fig. 2a). For example, sediments typically include a mix of in situ and reworked tests. That means “recent” sediments may contain a few shells from periods during which the configuration of low-oxygen waters may have been different from that in the past half-century. Where *G. hexagonus* tests are found below modern well-oxygenated waters, the species does not exceed 1% of the assemblage (Supplementary Fig. 1). Thus, for a study particularly sensitive to uncertainty arising from false positives, an abundance metric rather than binary presence/absence could be an alternate approach. By contrast, the relative rarity of *G. hexagonus* means that false negatives are probably far more common. In a standard assemblage of 300 individuals, species with a relative abundance <0.3% are likely to go unobserved. This could be a significant source of error for rare species such as *G. hexagonus*, especially at highly productive sites where surface-dwelling foraminifera far outnumber OMZ-affiliated species living at depth. This would be compounded by a bias of human identification away from rare species⁴⁷. For these reasons, the absence of *G. hexagonus* alone in most assemblages, should not be interpreted as a conclusive indicator of a well-oxygenated water column. Absences are only interpreted here in large assemblages (>1800 individuals

counted), if replicated across multiple sites, or supported by Community Earth System Model (CESM) outputs.

Distribution of OMZs in the Pliocene

The presence (or absence) of *G. hexagonus* remains largely constant through the Pliocene in deep sea sites from the Pacific, Indian, and Eastern Atlantic oceans (Fig. 4). This is supported by a biogeochemically enabled CESM simulation with an active PMOC and ocean biogeochemistry which predicts low-oxygen mid-waters through all three regions. All reported presences of Pliocene *G. hexagonus* fall within a grid square of low-oxygen mid-waters in the CESM simulation (Fig. 2b; Supplementary Fig. 2). Application of our SDM to the oxygen output from this Pliocene-like CESM simulation indicates suitable habitat for *G. hexagonus* in most low-oxygen mid-waters of the subpolar to tropical regions, with greater suitability around the Equator and in the Southern Hemisphere (Fig. 2b).

The global configuration of Pliocene OMZs inferred from the distribution of *G. hexagonus* and Pliocene-like CESM simulation are broadly similar to modern, with the noteworthy distinction that the

Pliocene hosted a greater expanse of low-oxygen waters in the North Atlantic and less in the North Pacific. We note that neither proxy nor model capture high-frequency oceanographic variability on orbital or shorter timescales that could have impacted OMZ distribution over the course of the Pliocene. Thus, the distribution of OMZs described here can be considered a baseline for the distribution of low-oxygen mid-waters given Pliocene climate and circulation parameters.

Eastern Boundary Currents and evidence for PMOC

Most modern OMZ regions also supported OMZs during the Pliocene. This is despite evidence for less vigorous upwelling-conductive winds and reduced productivity in several key Pliocene EBUSs^{28,30–32}. Both the distribution of *G. hexagonus* and the Pliocene-like simulation suggest that at least two EBUSs, the Canary Current System in the eastern North Atlantic and the Humboldt (Peru) Current System in the eastern South Pacific, hosted low-oxygen mid-waters during the Pliocene. This demonstrates the importance of the confluence of low-oxygen source waters with upwelling-driven productivity for fueling OMZs in the Pliocene as in the modern ocean. The CESM output also predicts a

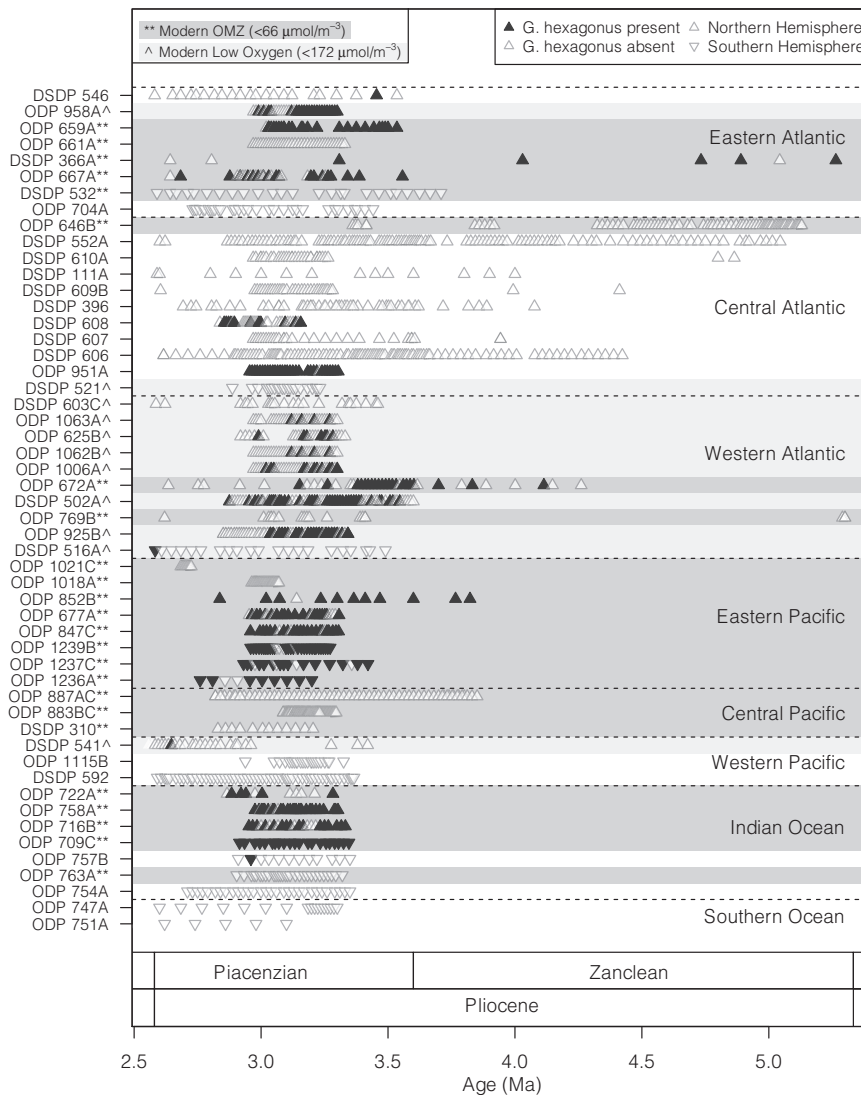


Fig. 4 | Presence/absence of *G. hexagonus* shells through time. Samples where *G. hexagonus* was present in the PRISM database are shown as filled black triangles; samples where *G. hexagonus* was not found are open gray triangles⁴¹. Records are organized by region. Sites highlighted by a dark gray box and labeled with a “*” in the y-axis legend are clearly associated with a modern OMZ and

oxygen <66 μmol m⁻³. Those with a light gray box and labeled with a “*” in the legend are regions which meet our low-oxygen threshold (<172 μmol m⁻³; Fig. 1) but are not consistently understood to be within permanent modern OMZ. Upward-facing triangles are from sites in the northern hemisphere, while downward-facing triangles indicate sites in the southern hemisphere.

low-oxygen region associated with the Benguela Current System in the eastern South Atlantic (Fig. 2b), which our SDM would affirm as suitable habitat for *G. hexagonus* in the Pliocene (Fig. 3b). However, there are no sites in the PRISM database to corroborate the models in this region (Figs. 2b and 3b), with the closest site, DSDP 532, showing *G. hexagonus* absent.

While most EBUSs appear to host an OMZ during the Pliocene, *G. hexagonus* is conspicuously absent from Northeast Pacific sites ODP 1021 and 1018 (California Current), both of which underlie a large, established OMZ today. A better oxygenated Northeast Pacific is supported by $\delta^{15}\text{N}$ records from California Margin site ODP 1012, which records relatively little denitrification in the Eastern Tropical North Pacific until -2.1 Ma^{31} . Benthic $\delta^{13}\text{C}$ records from the Southern California margin also indicate more vigorous circulation and increased ventilation⁴⁸. The inference of a relatively well-oxygenated Pliocene California Current System is consistent with the Pliocene-like CEM output due to its simulation of PMOC. Under a PMOC regime both the age and path of intermediate waters circulating through the Pacific

would be substantially different from the present day, leading to younger, more oxygen-rich waters being upwelled into the California Current System (Fig. 5).

In the Pliocene-like simulation with PMOC, the Southern Ocean is the endpoint for waters subducted in both the North Pacific and Atlantic. One consequence of this is an increase in Pacific-sourced waters with 100 to 1000 year transit times in the Southern Ocean⁴⁹, and thus an older, more oxygen-depleted Southern hemisphere. Despite low-oxygen mid-waters creating suitable habitat in the Southern Ocean (Fig. 3b), *G. hexagonus* is entirely absent (Fig. 2b). We hypothesize that *G. hexagonus* was excluded from the Southern Ocean due to geographic limitations noted above with regards to the modern subpolar North Pacific. Other alternatives are possible, including that the Pliocene-like simulation predicts a greater degree of oxygen-depletion than was present, but this would need to be tested using alternate proxy approaches.

The Eastern Equatorial Pacific (EEP), associated with the Eastern Pacific cold tongue, is the site of the greatest expanse of low oxygen

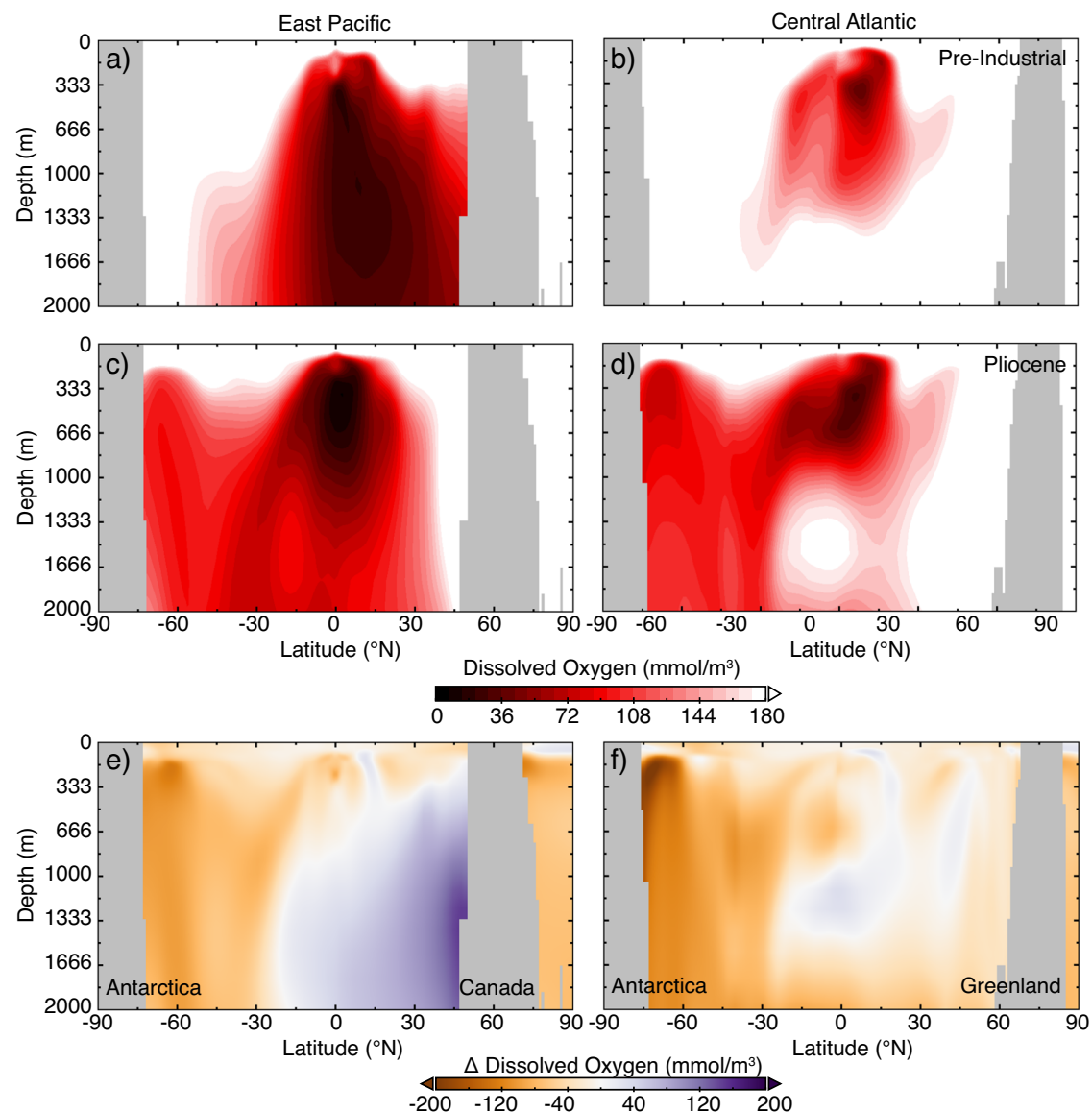


Fig. 5 | Comparison of oxygen in sections from Pre-Industrial and Pliocene-like simulations. Transects through the East Pacific (130°W) (a, c, e) and Central Atlantic (30°W) (b, d, f) with outputs from the Pre-Industrial control (a, b) and Pliocene-like simulation (c, d), and the difference in oxygenation between the

Pliocene and Pre-Industrial (e, f) from 0 to 2000 m. Locations of transects are shown in Fig. 1. See Supplementary Fig. 6 to compare modern observational data to the Pre-Industrial control.

waters in the modern ocean, driven by both high productivity and low ventilation^{17,50}. Our results affirm that an OMZ persisted in this region during the Pliocene. The Pliocene EEP is widely reported to have had a reduced east-west temperature gradient^{51,52}, with some authors interpreting warmer EEP temperatures as a decrease in upwelling, implying reduced productivity and thus subsurface respiration compared to today. While some records do show a decrease in EEP productivity centered on the mid-Pliocene⁵³, others demonstrate sustained productivity and oxygen-depleted intermediate waters, akin to modern dynamics^{54,55}. Warmer Pliocene EEP temperatures could also reflect an altered source of warmer sub-thermocline waters, a hypothesis broadly supported by subsurface temperature proxies⁵⁶, regional pH proxies⁵⁷, and our finding of a low-oxygen water mass occupying EEP mid-waters (Fig. 2).

In addition to the Atlantic and Pacific Ocean EBUS-associated OMZs, there is widespread evidence from sediment geochemistry and benthic foraminiferal assemblages for increased productivity and reducing conditions in the Indian Ocean from the late-Miocene through mid-Pliocene (-6.5-3 Ma), including a potentially expanded OMZ relative to the Pleistocene⁵⁸⁻⁶¹. A strong, Indian Ocean OMZ is supported by the presence of *G. hexagonus* in the northern Indian Ocean during the Pliocene and the modeled extent of low oxygen conditions (Fig. 2b), affirming previous work. This result is consistent with an influence of low-oxygen Southern Ocean-sourced waters during the Pliocene.

North Atlantic Pliocene OMZs

One striking difference between modern and Pliocene distributions of low-oxygen waters is in the western North Atlantic, including the Caribbean Sea and portions of the Subtropical Gyre. Both are regions with relatively high subsurface oxygen in the modern ocean but for which there is both proxy and model support for low-oxygen waters during the Pliocene. For much of the western North Atlantic, altered intermediate water circulation is the likely source of decreased oxygenation. These regions are currently ventilated by AAIW⁶². However this arrangement was preceded by a warmer, saltier, Pacific-sourced 'proto-AAIW' prior to ~3 Ma⁶³ with lower O₂ content. The presence of a poorly oxygenated proto-AAIW would have influenced the Canary Current System in the eastern North Atlantic, where modern AAIW is a significant contributor to OMZ depth and deeper (>600 m) waters⁶⁴. The potential for OMZ formation in the North Atlantic is particularly salient given observations of warming and deoxygenating source waters for these regions over the past decades¹¹.

There is substantial evidence for both high productivity and the presence of Western Atlantic OMZs in warm climates preceding the Pliocene, with benthic foraminiferal assemblages reflecting a well-developed OMZ in the western Caribbean in the late Miocene^{65,66}. While little direct evidence exists for a benthic OMZ persisting into the Pliocene, paleontological and geochemical records suggest a more productive Western Atlantic in the Pliocene relative to the Pleistocene. Ichthyofaunas reflect an upwelling ecosystem around the Cariaco trench⁶⁷, while ostracod assemblages indicate cooler, upwelling-associated temperatures along the Southwest Atlantic margin⁶⁸. In the eastern Gulf of Mexico, high mid-Pliocene productivity is associated with stronger-than-modern upwelling⁶⁹. Similarly, upwelling-associated planktic foraminifers *Neogloboquadrina pachyderma* and *Globigerina bulloides* are abundant in the Western Caribbean in the Late Pliocene^{70,71}. Trace elements, as well as CaCO₃ and SiO₂ mass accumulation rates from ODP Site 999 suggest heightened export productivity until -1.7 Ma⁷². At Ceara Rise ODP Site 925, elevated productivity compared to present day persisted until at least -3.7 Ma⁷³, while mid-Pliocene (-4-3 Ma) δ¹³C of thermocline dwelling *Neogloboquadrina dutertrei* is lower than either surface-dwelling *Trilobatus sacculifer* or Holocene *N. dutertrei*⁷⁴. Together, these lines of evidence

all indicate elevated Pliocene upwelling-driven productivity, consistent with the presence of an OMZ.

A shift from the presence to a consistent absence of *G. hexagonus* tests in several North Atlantic sites could suggest a regional change occurring during the mid-Piacenzian. The species apparently disappears from Northwest Atlantic ODP Sites 1063, 625, 672, and 925 in the Western Atlantic between 3.5 and 3 Ma, as well as from ODP Site 958 in the Eastern Atlantic (Fig. 4). While precise dating of this apparent shift is limited by data availability, the timing would be consistent with either an evolution of source-waters from a Pacific-influenced proto-AAIW to a more modern AAIW composition⁶³, or reduced upwelling and decreased productivity in the marginal Western Atlantic seas.

High productivity in the early and mid-Pliocene Western Atlantic has traditionally been attributed to the inflow of more nutrient-rich waters across the Central American Seaway⁷⁵. The aftermath of seaway closure is linked with the development of the Western Atlantic Warm Pool⁷⁶, which decreased productivity and facilitated the expansion of reef ecosystems throughout the Caribbean^{77,78}. The timing of Central American Seaway closure remains debated⁷⁹. Geochemical differentiation of surface waters likely began as early as -4.2 Ma⁸⁰ with the development of a warm pool by 4 Ma⁷⁶, and an increasingly oligotrophic Caribbean emerging between 4.2-2.5 Ma⁸¹. However, other authors show potentially intermittent surface connectivity persisted until as recently as 3-2.5 Ma⁷⁹. Notably, the CESM used here is parameterized with a fully formed Panama Isthmus. Thus, while the Central American Seaway may have contributed to increased productivity and remineralization in the Pliocene Western Atlantic, it appears not to be a necessary condition for circulatory changes that may produce a Western Atlantic OMZ (Figs. 2, 5). This finding has particular significance for the future ocean, as Southern Ocean-sourced intermediate waters in the Atlantic have been deoxygenating since the mid 20th century¹¹. Thus, the Pliocene may offer a meaningful reference point, demonstrating the potential for Atlantic OMZ expansion, with a modern continental configuration.

Warm, poorly ventilated mid-waters allowed for widespread OMZs in the Pliocene as evidenced by the distribution of the low-oxygen affiliated species *G. hexagonus* and supported by both Earth System and Species Distribution Models. This includes maintenance of low-oxygen waters underlying the Humboldt Current System in the eastern South Pacific and the northern Indian Ocean similar to modern day. Low-oxygen mid-waters were also pervasive in the North Atlantic through the mid-Piacenzian, reflecting an evolution from a proto-AAIW water mass to a modern, better oxygenated intermediate water configuration in the Late Pliocene. In contrast to the modern ocean, the Pliocene California Current EBUS appeared well-oxygenated, consistent with altered intermediate water circulation associated with a Pliocene PMOC. Thus, a warmer world can support both regionally expanded and contracted OMZs, influenced by distant intermediate water formation and circulation. The close ties between *G. hexagonus* and modern OMZs and the striking data-model match found here, suggest that the species has enormous potential to reveal the presence and evolution of pelagic low-oxygen water masses.

Methods

There is no single definition of an OMZ, with quantitative thresholds varying between contexts and studies. Here, we account for regions where waters shallower than 1000 m reach oxygen concentrations of 172 μmol m⁻³ or less (Fig. 1). This value has been chosen to be inclusive of all major regions of the modern ocean that are frequently described as possessing an OMZ and to account for differences in OMZ depth (Supplementary Fig. 2). Unless otherwise stated, O₂ maps were made with the use of NASA's "Earth" overlay (<https://www.giss.nasa.gov/tools/panoply/>).

Presence of *G. hexagonus*

The distribution of *G. hexagonus* tests in marine sediments is used as an indicator of overlying oxygen-depleted mid-waters in the Pliocene. We interpret data only in terms of presence/absence. This has been done in part to account for unconstrained differences in sedimentation rate and preservation between sites. Moreover, modern observations show that *G. hexagonus* is likely not sharing a habitat with the planktic foraminifera species abundant above the oxycline³⁷. Due to this fundamental difference in habitat and very low densities of *G. hexagonus* in the modern ocean³⁷, metrics such as relative abundance will be at least as responsive to varying abundances of shallow-dwelling species as mid-water species such as *G. hexagonus*.

The presence or absence of *G. hexagonus* in the Pliocene was assessed based on a database of planktic foraminifera faunas published as a part of the PRISM project⁴¹. The PRISM project focuses on the mid-Piacenzian Warm Period (~3.3–3.0 Ma), with the largest density of samples clustered around this interval⁴¹, but contains samples dated from 6.2 to 1.8 Ma. Only data from the Pliocene (5.3–2.6 Ma) is included here (Fig. 4). A modern comparison draws on faunas from the Brown University Database (BFD) and ForCenS Database of recent sediments^{42,43}, and reports from plankton tows and sediment traps^{37–40,82–87} (Supplementary Figs. 1, 3). Given the relative rarity of *G. hexagonus* in both modern and Pliocene sediments (<3%), absences are considered meaningful only if counts at a site are sufficient to capture a relative abundance of at least 0.1%. One outcome of this threshold is that absences from “modern” sites (~300 count/site in ForCenS) are not formally considered, while they are from the PRISM database (>1800 count/site).

Ecological modeling of *G. hexagonus*

The distribution of *G. hexagonus* in the modern ocean along with physical and biogeochemical environmental conditions and a variety of statistical/machine learning algorithms was used to estimate *G. hexagonus* habitat suitability in the modern ocean. This ecological model was then driven by corresponding environmental variables from a simulated Pliocene-like ocean (see next section) to project habitat suitability under Pliocene conditions. Data for *G. hexagonus* occurrence in the modern ocean was taken from the BFD (Atlantic only) and ForCenS (other basins) Databases^{42,43} and converted to presence/absence (Fig. 2a; Supplementary Fig. 3). The use of the BFD in the Atlantic was chosen so as not to presuppose the absence of *G. hexagonus* from this basin in our models.

Modern environmental covariate data, including temperature⁸⁸, salinity⁸⁹, dissolved oxygen⁹⁰ nitrate, phosphate, and silica⁹¹ were taken from WOAI8 at depths ranging from 0–1000 m. SDMs were constructed from the relationship between occurrence (presence only) and environmental covariate data using a variety of statistical (logistic regression, General Additive Models) and machine learning (Boosted Regression Trees, Random Forests, Maximum Entropy) algorithms commonly employed in SDMs⁹². Each model was run multiple times with 5-fold cross validation to assess performance and robustness. Models using both all variables and dissolved oxygen only were constructed and compared.

Physical and biogeochemical modeling of Pliocene conditions

This study makes use of Pre-Industrial and Early (~4–5 Ma) Pliocene-like climate simulations performed using the coupled ocean-atmosphere Community Earth System Model (CESM) version 1.2.2. While a detailed description of these simulations is provided elsewhere⁵⁷, we will briefly summarize here. These simulations have active ocean biogeochemistry⁹³ and use the T31 gx3v7 configuration designed for long paleoclimate simulations⁹⁴. In our case these have been run for 3000 years, allowing the ocean to reach quasi-equilibrium⁵⁷ (Supplementary Fig. 3). The atmospheric (Community Atmosphere Model 4)

and land surface components (Community Land Model 4) have a spectral truncation of T31, and the oceanic (Parallel Ocean Program 2) and sea ice components (Community Ice Code) have a resolution ranging from 3° near the poles to 1° at the equator. The design for the Pre-Industrial experiment consists simply of the default B₁₈₅₀BGC-BDRD CESM component set (Supplementary Fig. 4). For the Pliocene experiment, cloud albedo is reduced in the extratropics and increased in the tropics by modifying the liquid and ice water path in the shortwave radiation scheme following the design of^{25,44,45}. All other boundary conditions and radiative forcings in the Pliocene experiment are the same as the Pre-Industrial control. The modifications to cloud shortwave radiative forcing lead to large-scale warming patterns that largely reproduce the meridional and zonal gradients seen in Pliocene SST reconstructions^{45,95}. These ocean warming patterns in turn influence the large-scale hydrological cycle²⁸ which has important implications for the density of surface waters in the subpolar North Pacific leading to deep water formation and a PMOC, which influences oxygen^{25,57} (Supplementary Figs. 5, 6). The analysis presented here is based on the last 100 years of each simulation (years 2901–3000).

Data availability

All data associated with this manuscript have been previously published and is freely available as part of the PRISM (<https://www.ncei.noaa.gov/access/paleo-search/study/19281>), ForCenS (<https://doi.org/10.1594/PANGAEA.873570>), and Brown Foraminiferal Databases (<https://doi.org/10.1594/PANGAEA.96900>). Model outputs are available at XXXX.

Code availability

Climate simulation and habitat suitability output data for this study will be uploaded to Zenodo (<https://zenodo.org/deposit/7254850>).

References

- Chan, F. et al. Emergence of Anoxia in the California Current Large Marine Ecosystem. *Science* **319**, 920 (2008).
- Gruber, N. The marine nitrogen cycle: overview and challenges. *Nitrogen Mar. Environ.* **2**, 1–50 (2008).
- Stramma, L., Johnson, G. C., Firing, E. & Schmidtko, S. Eastern Pacific oxygen minimum zones: Supply paths and multidecadal changes. *Journal of Geophysical Research: Oceans* **115**, <https://doi.org/10.1029/2009JC005976> (2010).
- Stramma, L. et al. Expansion of oxygen minimum zones may reduce available habitat for tropical pelagic fishes. *Nat. Clim. Change* **2**, 33–37 (2012).
- DeVries, T., Deutsch, C., Primeau, F., Chang, B. & Devol, A. Global rates of water-column denitrification derived from nitrogen gas measurements. *Nat. Geosci.* **5**, 547–550 (2012).
- Breitburg, D. et al. Declining oxygen in the global ocean and coastal waters. *Science* **359**, 6371–6383 (2018).
- Levin, L. Manifestation, Drivers, and Emergence of Open Ocean Deoxygenation. *Annu. Rev. Mar. Sci.* **10**, 229–260 (2017).
- Diaz, R. J. & Rosenberg, R. Spreading dead zones and consequences for marine ecosystems. *Science* **321**, 926–929 (2008).
- Stramma, L., Schmidtko, S., Levin, L. A. & Johnson, G. C. Ocean oxygen minima expansions and their biological impacts. *Deep Sea Res. Part I: Oceanographic Res. Pap.* **57**, 587–595 (2010).
- Keeling, R. F., Körtzinger, A. & Gruber, N. Ocean deoxygenation in a warming world. *Annu. Rev. Mar. Sci.* **2**, 199–229 (2010).
- Schmidtko, S., Stramma, L. & Visbeck, M. Decline in global oceanic oxygen content during the past five decades. *Nature* **542**, 335–339 (2017).
- Cannariato, K. G., Kennett, J. P. & Behl, R. J. Biotic response to late Quaternary rapid climate switches in Santa Barbara Basin: Ecological and evolutionary implications. *Geology* **27**, 63–66 (1999).

13. van Geen, A. et al. On the preservation of laminated sediments along the western margin of North America. *Paleoceanography* **18**, 4 (2003).
14. Nameroff, T. J., Calvert, S. E. & Murray, J. W. Glacial-interglacial variability in the eastern tropical North Pacific oxygen minimum zone recorded by redox-sensitive trace metals. *Paleoceanography* **19**, PA1010 (2004).
15. Moffitt, S. E. et al. Paleoceanographic insights on recent oxygen minimum zone expansion: Lessons for modern oceanography. *PLoS One* **10**, e0115246 (2015).
16. Hendy, I. & Pedersen, T. Oxygen minimum zone expansion in the eastern tropical North Pacific during deglaciation. *Geophys. Res. Lett.* **33**, 20 (2006).
17. Paulmier, A. & Ruiz-Pino, D. Oxygen minimum zones (OMZs) in the modern ocean. *Prog. Oceanogr.* **80**, 113–128 (2009).
18. Pagani, M., Liu, Z., LaRiviere, J. & Ravelo, A. C. High Earth-system climate sensitivity determined from Pliocene carbon dioxide concentrations. *Nat. Geosci.* **3**, 27–30 (2010).
19. Seki, O. et al. Alkenone and boron-based Pliocene pCO_2 records. *Earth Planet. Sci. Lett.* **292**, 201–211 (2010).
20. Martinez-Botí, M. A. et al. Plio-Pleistocene climate sensitivity evaluated using high-resolution CO₂ records. *Nature* **518**, 49–54 (2015).
21. Dowsett, H., Robinson, M. & Foley, K. Pliocene three-dimensional global ocean temperature reconstruction. *Climate* **5**, 769–783 (2009).
22. Haywood, A. M. et al. Introduction. Pliocene climate, processes and problems. *Philos. Trans. R. Soc. A: Math., Phys. Eng. Sci.* **367**, 3–17 (2009).
23. Haywood, A. M. et al. The Pliocene Model Intercomparison Project Phase 2: large-scale climate features and climate sensitivity. *Climate* **16**, 2095–2123 (2020).
24. Dowsett, H. J. et al. The PRISM (Pliocene palaeoclimate) reconstruction: time for a paradigm shift. *Philos. Trans. R. Soc. A: Math., Phys. Eng. Sci.* **371**, 20120524 (2013).
25. Burls, N. J. et al. Active Pacific meridional overturning circulation (PMOC) during the warm Pliocene. *Sci. Adv.* **3**, e1700156 (2017).
26. Ford, H. L. et al. Sustained mid-Pliocene warmth led to deep water formation in the North Pacific. *Nat. Geosci.* **15**, 658–663 (2022).
27. Arnold, N. P. & Tziperman, E. Reductions in midlatitude upwelling-favorable winds implied by weaker large-scale Pliocene SST gradients. *Paleoceanography* **31**, 27–39 (2016).
28. Burls, N. J. & Fedorov, A. V. Wetter subtropics in a warmer world: Contrasting past and future hydrological cycles. *Proc. Natl Acad. Sci.* **114**, 12888–12893 (2017).
29. Etourneau, J., Martinez, P., Blanz, T. & Schneider, R. Pliocene–Pleistocene variability of upwelling activity, productivity, and nutrient cycling in the Benguela region. *Geology* **37**, 871–874 (2009).
30. Marlow, J. R., Lange, C. B., Wefer, G. & Rosell-Melé, A. Upwelling intensification as part of the Pliocene–Pleistocene climate transition. *Science* **290**, 2288–2291 (2000).
31. Liu, Z., Altabet, M. A. & Herbert, T. D. Plio-Pleistocene denitrification in the eastern tropical North Pacific: Intensification at 2.1 Ma. *Geochem., Geophysics, Geosystems* **9**, 11 (2008).
32. Ravelo, A. et al. Pliocene carbonate accumulation along the California margin. *Paleoceanography* **12**, 729–741 (1997).
33. Brierley, C. M. & Fedorov, A. V. Comparing the impacts of Miocene–Pliocene changes in inter-ocean gateways on climate: Central American Seaway, Bering Strait, and Indonesia. *Earth Planet. Sci. Lett.* **444**, 116–130 (2016).
34. Jenkyns, H. C. Cretaceous anoxic events: from continents to oceans. *J. Geol. Soc.* **137**, 171–188 (1980).
35. Jenkyns, H. C. Geochemistry of oceanic anoxic events. *Geochemistry, Geophysics, Geosystems* **11**, <https://doi.org/10.1029/2009GC002788> (2010).
36. Schlanger, S. O. & Jenkyns, H. Cretaceous oceanic anoxic events: causes and consequences. *Neth. J. Geosci./Geologie en. Mijnb.* **55**, 3 (2007).
37. Davis, C. V., Wishner, K., Renema, W. & Hull, P. M. Vertical distribution of planktic foraminifera through an oxygen minimum zone: how assemblages and test morphology reflect oxygen concentrations. *Biogeosciences* **18**, 977–992 (2021).
38. Birch, H., Coxall, H. K., Pearson, P. N., Kroon, D. & O’Regan, M. Planktonic foraminifera stable isotopes and water column structure: Disentangling ecological signals. *Mar. Micropaleontol.* **101**, 127–145 (2013).
39. Fairbanks, R. G., Sverdløve, M., Free, R., Wiebe, P. H. & Bé, A. W. Vertical distribution and isotopic fractionation of living planktonic foraminifera from the Panama Basin. *Nature* **298**, 841–844 (1982).
40. Ortiz, J. D., Mix, A., Rugh, W., Watkins, J. & Collier, R. Deep-dwelling planktonic foraminifera of the northeastern Pacific Ocean reveal environmental control of oxygen and carbon isotopic disequilibria. *Geochimica et Cosmochimica Acta* **60**, 4509–4523 (1996).
41. Dowsett, H., Robinson, M. & Foley, K. A global planktic foraminifer census data set for the Pliocene ocean. *Sci. Data* **2**, 150076 (2015).
42. Prell, W. L., Martin, A., Cullen, J. L. & Trend, M. The Brown University Foraminiferal Data Base (BFD). *PANGAEA* <https://doi.org/10.1594/pangaea.96900> (1999)
43. Siccha, M. & Kucera, M. ForCenS, a curated database of planktonic foraminifera census counts in marine surface sediment samples. *Sci. Data* **4**, 170109 (2017).
44. Burls, N. J. & Fedorov, A. V. What Controls the Mean East–West Sea Surface Temperature Gradient in the Equatorial Pacific: The Role of Cloud Albedo. *J. Clim.* **27**, 2757–2778 (2014).
45. Burls, N. J. & Fedorov, A. V. Simulating Pliocene warmth and a permanent El Niño-like state: The role of cloud albedo. *Paleoceanography* **29**, 893–910 (2014).
46. Be, A. W. H. & Tolderlund D. S. Distribution and ecology of planktonic foraminifera. In: Funnell, B. M., Riedel, W. R. (Eds) *The Micropaleontology of Oceans*. Cambridge University Press, London, pp. 105–150 (1971).
47. Hsiang et al. Endless Forams: >34,000 modern planktonic foraminiferal images for taxonomic training and automated species recognition using convolutional neural networks. *Paleoceanogr. Palaeoclimatol.* **34**, 1157–1177 (2019).
48. Kwiec, P. & Ravelo, A. Pacific Ocean intermediate and deep water circulation during the Pliocene. *Palaeogeogr., Palaeoclimatol., Palaeoecol.* **154**, 191–217 (1999).
49. Thomas, M. D., Fedorov, A. V., Burls, N. J. & Liu, W. Oceanic pathways of an active Pacific Meridional Overturning Circulation (PMOC). *Geophys. Res. Lett.* **48**, e2020GL091935 (2021).
50. Fiedler, P. C. & Talley, L. D. Hydrography of the eastern tropical Pacific: A review. *Prog. Oceanogr.* **69**, 143–180 (2006).
51. Wara, M. W., Ravelo, A. C. & Delaney, M. L. Permanent El Niño-like conditions during the Pliocene warm period. *Science* **309**, 758–761 (2005).
52. Ravelo, A. C., Dekens, P. S. & McCarthy, M. Evidence for El Niño-like conditions during the Pliocene. *GSA Today* **16**, 4 (2006).
53. Lyle, M. & Baldauf, J. Biogenic sediment regimes in the Neogene equatorial Pacific, IODP Site U1338: Burial, production, and diatom community. *Palaeogeogr., Palaeoclimatol., Palaeoecol.* **433**, 106–128 (2015).
54. Kamikuri, S.-i., Motoyama, I., Nishi, H. & Iwai, M. Evolution of Eastern Pacific Warm Pool and upwelling processes since the middle Miocene based on analysis of radiolarian assemblages: Response to Indonesian and Central American Seaways. *Palaeogeogr., Palaeoclimatol., Palaeoecol.* **280**, 469–479 (2009).

55. Reghellin, D., Coxall, H. K., Dickens, G. R. & Backman, J. Carbon and oxygen isotopes of bulk carbonate in sediment deposited beneath the eastern equatorial Pacific over the last 8 million years. *Paleoceanography* **30**, 1261–1286 (2015).
56. Dekens, P. S., Ravelo, A. C. & McCarthy, M. D. Warm upwelling regions in the Pliocene warm period. *Paleoceanography* **22**, 3 (2007).
57. Shankle, M. G. et al. Pliocene decoupling of equatorial Pacific temperature and pH gradients. *Nature* **598**, 457–461 (2021).
58. Hermelin, J. Variations in the benthic foraminiferal fauna of the Arabian Sea: a response to changes in upwelling intensity? *Geological Society, London, Special Publications* **64**, 151–166 (1992).
59. Dickens, G. R. & Owen, R. M. Late Miocene-early Pliocene manganese redirection in the central Indian Ocean: Expansion of the intermediate water oxygen minimum zone. *Paleoceanography* **9**, 169–181 (1994).
60. Dickens, G. R. & Owen, R. M. The latest Miocene-early Pliocene biogenic bloom: a revised Indian Ocean perspective. *Mar. Geol.* **161**, 75–91 (1999).
61. Gupta, A. K. & Thomas, E. Latest Miocene-Pleistocene Productivity and Deep-Sea Ventilation in the Northwestern Indian Ocean (Deep Sea Drilling Project Site 219). *Paleoceanography* **14**, 62–73 (1999).
62. Talley, L. D. Some aspects of ocean heat transport by the shallow, intermediate and deep overturning circulations. *Geophys. Monogr.-Am. Geophys. Union* **112**, 1–22 (1999).
63. Karas, C., Goldstein, S. L. & deMenocal, P. B. Evolution of Antarctic Intermediate Water during the Plio-Pleistocene and implications for global climate: Evidence from the South Atlantic. *Quat. Sci. Rev.* **223**, 105945 (2019).
64. Santos, G. C., Kerr, R., Azevedo, J. L. L., Mendes, C. R. B. & da Cunha, L. C. Influence of Antarctic intermediate water on the deoxygenation of the Atlantic Ocean. *Dyn. Atmospheres Oceans* **76**, 72–82 (2016).
65. McLaughlin, P. P. & Gupta, Sen B. K. Benthic foraminiferal record in the Miocene-Pliocene sequence of the Azua Basin, Dominican Republic. *J. Foraminifer. Res.* **24**, 75–109 (1994).
66. Wilson, B. Benthonic foraminiferal paleoecology indicates an oxygen minimum zone and an allochthonous, inner neritic assemblage in the Brasso Formation (Middle Miocene) at St. Fabien Quarry, Trinidad, West Indies. *Caribb. J. Sci.* **44**, 228–235 (2008).
67. Aguilera, O. & De Aguilera, D. R. An exceptional coastal upwelling fish assemblage in the Caribbean Neogene. *J. Paleontol.* **75**, 732–742 (2001).
68. Cronin, T. M. Pliocene shallow water paleoceanography of the North Atlantic Ocean based on marine ostracodes. *Quat. Sci. Rev.* **10**, 175–188 (1991).
69. Allmon, W. D., Emslie, S. D., Jones, D. S. & Morgan, G. S. Late Neogene oceanographic change along Florida's west coast: evidence and mechanisms. *J. Geol.* **104**, 143–162 (1996).
70. Keigwin, L. D. Jr Pliocene closing of the Isthmus of Panama, based on biostratigraphic evidence from nearby Pacific Ocean and Caribbean Sea cores. *Geology* **6**, 630–634 (1978).
71. Keller, G., Zenker, C. E. & Stone, S. Late Neogene history of the Pacific-Caribbean gateway. *J. South Am. Earth Sci.* **2**, 73–108 (1989).
72. Trumbo, S. K. *Marine Export Productivity and the Demise of the Central American Seaway* MS thesis, University of California, San Diego, (2015).
73. Diester-Haass, L., Billups, K. & Emeis, K. C. In search of the late Miocene-early Pliocene “biogenic bloom” in the Atlantic Ocean (Ocean Drilling Program Sites 982, 925, and 1088). *Paleoceanography* **20**, <https://doi.org/10.1029/2005PA001139> (2005).
74. Billups, K., Ravelo, A. & Zachos, J. Early Pliocene climate: A perspective from the western equatorial Atlantic warm pool. *Paleoceanography* **13**, 459–470 (1998).
75. Jackson, J. B. & O’Dea, A. Timing of the oceanographic and biological isolation of the Caribbean Sea from the tropical eastern Pacific Ocean. *Bull. Mar. Sci.* **89**, 779–800 (2013).
76. Steph, S. et al. Early Pliocene increase in thermohaline overturning: A precondition for the development of the modern equatorial Pacific cold tongue. *Paleoceanography* **25**, 2 (2010).
77. Allmon, W. Nutrients, temperature, disturbance, and evolution: a model for the late Cenozoic marine record of the western Atlantic. *Palaeogeogr. Palaeoclimatol. Palaeoecol.* **166**, 9–26 (2001).
78. Leonard-Pingel, J. S., Jackson, J. B. & O’Dea, A. Changes in bivalve functional and assemblage ecology in response to environmental change in the Caribbean Neogene. *Paleobiology* **38**, 509–524 (2012).
79. O’Dea, A. et al. Formation of the Isthmus of Panama. *Sci. Adv.* **2**, e1600883 (2016).
80. Haug, G. H., Tiedemann, R., Zahn, R. & Ravelo, A. C. Role of Panama uplift on oceanic freshwater balance. *Geology* **29**, 207–210 (2001).
81. Jain, S. & Collins, L. S. Trends in Caribbean paleoproductivity related to the Neogene closure of the Central American Seaway. *Mar. Micropaleontol.* **63**, 57–74 (2007).
82. Sautter, L. R. & Thunell, R. C. Planktonic foraminiferal response to upwelling and seasonal hydrographic conditions; sediment trap results from San Pedro Basin, Southern California Bight. *J. Foraminifer. Res.* **21**, 347–363 (1991).
83. Davis, C. V., Hill, T. M., Russell, A. D., Gaylord, B. & Jahncke, J. Seasonality in planktic foraminifera of the central California coastal upwelling region. *Biogeosciences* **13**, 5139 (2016).
84. Marchant, M., Hebbeln, D. & Wefer, G. Seasonal flux patterns of planktic foraminifera in the Peru-Chile current. *Deep Sea Res. Part I: Oceanographic Res. Pap.* **45**, 1161–1185 (1998).
85. Rao, K. K., Jayalakshmy, K., Kumaran, S., Balasubramanian, T. & Kutty, M. K. Planktonic foraminifera in waters off the Coromandel coast, Bay of Bengal. (1989).
86. Rippert, N. et al. Constraining foraminiferal calcification depths in the western Pacific warm pool. *Mar. Micropaleontol.* **128**, 14–27 (2016).
87. Smart, S. M. et al. Ground-truthing the planktic foraminifer-bound nitrogen isotope paleo-proxy in the Sargasso Sea. *Geochimica et Cosmochimica Acta* **235**, 463–482 (2018).
88. Locarnini, M. et al. World ocean atlas 2018, volume 1: Temperature. (2018).
89. Zweng, M. et al. World ocean atlas 2018, volume 2: Salinity. (2019).
90. Garcia, H. et al. World Ocean Atlas 2018, Volume 3: Dissolved Oxygen, Apparent Oxygen Utilization, and Dissolved Oxygen Saturation. (2019).
91. Garcia, H. et al. World ocean atlas 2018. Vol. 4: Dissolved inorganic nutrients (phosphate, nitrate and nitrate+ nitrite, silicate). (2019).
92. Hijmans, R. J., & Elith, J. Species Distribution Models (2021).
93. Moore, J. K., Doney, S. C. & Lindsay, K. Upper ocean ecosystem dynamics and iron cycling in a global three-dimensional model. *Glob. Biogeochemical Cycles* **18**, 4 (2004).
94. Shields, C. A. et al. The low-resolution CCSM4. *J. Clim.* **25**, 3993–4014 (2012).
95. Fedorov, A. V., Burls, N. J., Lawrence, K. T. & Peterson, L. C. Tightly linked zonal and meridional sea surface temperature gradients over the past five million years. *Nat. Geosci.* **8**, 975–980 (2015).

Acknowledgements

This work was supported by National Science Foundation OCE-1851589 to CVD. A Hutchinson Postdoctoral Fellowship from the Yale Institution of Biospheric Studies supported ECS. We acknowledge high-performance computing support from Cheyenne (<https://doi.org/10.5065/D6RX99HX>) provided by NCAR’s Computational and Information Systems Laboratory, sponsored by

the NSF. This work was supported by National Science Foundation OCE-1844380 and OCE-2002448 to N.J.B.

Author contributions

CVD, ES, and PH conceived of the study; NB and PJ provided model simulations; CVD and ES carried out initial data analyses; CVD and ES wrote the initial manuscript draft and all authors contributed substantially to the final manuscript.

Competing interests

The authors declare no competing interests.

Additional information

Supplementary information The online version contains supplementary material available at <https://doi.org/10.1038/s41467-022-35083-x>.

Correspondence and requests for materials should be addressed to Catherine V. Davis.

Peer review information *Nature Communications* thanks Babette Hoogakker, Zunli Lu and the other, anonymous, reviewer(s) for their contribution to the peer review of this work.

Reprints and permissions information is available at <http://www.nature.com/reprints>

Publisher's note Springer Nature remains neutral with regard to jurisdictional claims in published maps and institutional affiliations.

Open Access This article is licensed under a Creative Commons Attribution 4.0 International License, which permits use, sharing, adaptation, distribution and reproduction in any medium or format, as long as you give appropriate credit to the original author(s) and the source, provide a link to the Creative Commons license, and indicate if changes were made. The images or other third party material in this article are included in the article's Creative Commons license, unless indicated otherwise in a credit line to the material. If material is not included in the article's Creative Commons license and your intended use is not permitted by statutory regulation or exceeds the permitted use, you will need to obtain permission directly from the copyright holder. To view a copy of this license, visit <http://creativecommons.org/licenses/by/4.0/>.

© The Author(s) 2023